Predicting the $B \to K^*$ form factors in light-cone QCD

M. Ahmady and R. Campbell

*Department of Physics, Mount Allison University, Sackville, N-B. E46 1E6, Canada**

S. Lord

Département de Mathématiques et Statistique,

Université de Moncton, Moncton, N-B. E1A 3E9, Canada†

R. Sandapen

Département de Physique et d'Astronomie,

Université de Moncton, Moncton, N-B. E1A 3E9, Canada &

Department of Physics, Mount Allison University, Sackville, N-B. E46 1E6, Canada ‡

arXiv:1401.6707v1 [hep-ph] 26 Jan 2014

We use QCD light-cone sum rules with holographic anti de Sitter/Chromodynamics (AdS/QCD) Distribution Amplitudes (DAs) for the K^* meson in order to predict the full set of seven $B \to K^*$ transition form factors for intermediate-to-high recoil of the vector meson. We provide simple parametrizations for the form factors that fit our AdS/QCD predictions. We also provide parametrizations that fit both our AdS/QCD predictions and the most recent lattice data for low recoil. We use our form factors to predict the differential and total branching fraction of the rare dileptonic decay $B \to K^* \mu^+ \mu^-$ which we compare to the recent LHCb data.

I. INTRODUCTION

B meson decays to $K^{(*)}$ are mediated by the penguin-induced flavor changing neutral current $b \to s$ transition which is an excellent venue for precision tests of the Standard Model (SM) and for probing new physics beyond the SM. Moreover, three-body decays like

*Electronic address: mahmady@mta.ca,recampbell@mta.ca

†Electronic address: esl8420@umoncton.ca

‡Electronic address: ruben.sandapen@umoncton.ca

$B \to K^*(\to K\pi)l^+l^-$ provide a plethora of angular observables, some of which may be sensitive to new physics. These considerations, along with the fact that the LHCb detector has a high efficiency in detecting muons, explains the fact that the decay $B \to K^*\mu^+\mu^-$ is presently generating a great deal of experimental [1–7] and theoretical [8–14] activity.

In a previous paper [15], we derived four holographic AdS/QCD DAs for the K^* meson: two twist-2 DAs, one for each polarization of the K^*; and two twist-3 DAs, vector and axial vector, for the transversely polarized K^*. We used the transverse DAs in order to predict the branching ratio and the power-suppressed isospin asymmetry of the radiative decay $B \to K^*\gamma$. We found that the transverse twist-2 AdS/QCD DA offers an advantage in that it avoids the end-point divergence encountered when computing the isospin asymmetry using the transverse twist-2 sum rules DA. Our predictions were consistent with experiment [15].

Our goal in this paper is to use both the longitudinal and transverse twist-2 AdS/QCD DAs in QCD light-cone sum rules [16–18] in order to compute the seven $B \to K^*$ transition form factors[35]. We shall then use these form factors to predict the differential branching ratio of the dileptonic decay $B \to K^*\mu^+\mu^-$ which we shall compare with the recent data released by the LHCb collaboration [5, 7]. The angular analysis of this decay is particularly interesting since the LHCb collaboration recently reported [4] a 3.7σ discrepancy between one angular observable at high recoil and the Standard Model prediction of Ref. [11] . Unlike the differential branching fraction, this particular angular observable is largely free from the hadronic uncertainties related to the form factors. It is not yet clear whether this discrepancy is caused by new physics or is due to statistical fluctuations and/or other theoretical uncertainties [10]. If the LHCb anomaly is due to new physics phenomena, they could perhaps be revealed in other observables including the differential and total branching fraction, provided we have a good understanding of the uncertainties in the $B \to K^*$ form factors.

II. FORM FACTORS

The seven $B \to K^*$ transition form factors $V, A_0, A_1, A_2, T_1, T_2$ and T_3 are defined by the following expressions [19]:

$$\begin{aligned}\langle K^*(k,\varepsilon)|\bar{s}\gamma^\mu(1-\gamma^5)b|B(p)\rangle &= \frac{2iV(q^2)}{m_B+m_{K^*}}\epsilon^{\mu\nu\rho\sigma}\varepsilon^*_\nu k_\rho p_\sigma - 2m_{K^*}A_0(q^2)\frac{\varepsilon^*\cdot q}{q^2}q^\mu \\ &- (m_B+m_{K^*})A_1(q^2)\left(\varepsilon^{\mu *}-\frac{\varepsilon^*\cdot q q^\mu}{q^2}\right) \\ &+ A_2(q^2)\frac{\varepsilon^*\cdot q}{m_B+m_{K^*}}\left[(p+k)^\mu - \frac{m_B^2-m_{K^*}}{q^2}q^\mu\right] \qquad (1)\end{aligned}$$

and

$$\begin{aligned}q_\nu\langle K^*(k,\varepsilon)|\bar{s}\sigma^{\mu\nu}(1-\gamma^5)b|B(p)\rangle &= 2T_1(q^2)\epsilon^{\mu\nu\rho\sigma}\varepsilon^*_\nu p_\rho k_\sigma \\ &- iT_2(q^2)[(\varepsilon^*\cdot q)(p+k)_\mu - \varepsilon^*_\mu(m_B^2-m_{K^*}^2)] \\ &- iT_3(q^2)(\varepsilon^*\cdot q)\left[\frac{q^2}{m_B^2-m_{K^*}^2}(p+k)_\mu - q_\mu\right] \qquad (2)\end{aligned}$$

where $q = p - k$ is the 4-momentum transfer and ε is the polarization 4-vector of the K^*.

At low-to-intermediate values of q^2, these form factors can be computed using QCD light-cone sum rules [16–18] . Here we shall use the light-cone sum rules derived in Ref. [17]:

$$\begin{aligned}V(q^2) &= \left(\frac{m_B+m_{K^*}}{2}\right)\left(\frac{m_b}{f_B m_B^2}\right)\exp\left(\frac{m_B^2}{M^2}\right)\int_\delta^1 \text{ụ}\,\exp\left(-\frac{m_b^2+p^2u\bar{u}-q^2\bar{u}}{uM^2}\right) \\ &\times\left\{m_b m_{K^*}\frac{f_{K^*}g_\perp^{(a)}(u)}{2u^2M^2}+\frac{f_{K^*}^\perp\phi_\perp(u)}{u}\right\}, \qquad (3)\end{aligned}$$

$$\begin{aligned}A_1(q^2) &= \left(\frac{1}{m_B+m_{K^*}}\right)\left(\frac{m_b}{f_B m_B^2}\right)\exp\left(\frac{m_B^2}{M^2}\right)\int_\delta^1 \text{ụ}\,\exp\left(-\frac{m_b^2+p^2u\bar{u}-q^2\bar{u}}{uM^2}\right) \\ &\times\left\{m_b m_{K^*}\frac{f_{K^*}g_\perp^{(v)}(u)}{u}+\frac{(m_b^2-q^2+p^2u^2)f_{K^*}^\perp\phi_\perp(u)}{2u^2}\right\}, \qquad (4)\end{aligned}$$

$$\begin{aligned}A_2(q^2) &= -(m_B+m_{K^*})\left(\frac{m_b}{f_B m_B^2}\right)\exp\left(\frac{m_B^2}{M^2}\right)\int_\delta^1 \text{ụ}\,\exp\left(-\frac{m_b^2+p^2u\bar{u}-q^2\bar{u}}{uM^2}\right) \\ &\times\left\{-\frac{m_b m_{K^*}}{u^2M^2}f_{K^*}\Phi_\parallel(u)-\frac{1}{2}\frac{f_{K^*}^\perp\phi_\perp(u)}{u}\right\}, \qquad (5)\end{aligned}$$

$$\begin{aligned}T_1(q^2) &= \frac{1}{4}\left(\frac{m_b}{f_B m_B^2}\right)\exp\left(\frac{m_B^2}{M^2}\right)\int_\delta^1 \frac{\text{u}}{\dot{u}}\,\exp\left(-\frac{m_b^2+p^2u\bar{u}-q^2\bar{u}}{uM^2}\right)\left\{m_b f_{K^*}^\perp\phi_\perp(u)+\right. \\ &\left. f_{K^*}m_{K^*}\left[\Phi_\parallel(u)+ug_\perp^{(v)}(u)+\frac{g_\perp^{(a)}(u)}{4}+\frac{(m_b^2+q^2-p^2u^2)g_\perp^a(u)}{4uM^2}\right]\right\}, \qquad (6)\end{aligned}$$

$$T_2(q^2) = \left(\frac{1}{2(m_{B^*}^2 - m_{K^*}^2)}\right)\left(\frac{m_b}{f_B m_B^2}\right)\exp\left(\frac{m_B^2}{M^2}\right)\int_\delta^1 \frac{du}{u}\exp\left(-\frac{m_b^2 + p^2 u\bar{u} - q^2\bar{u}}{uM^2}\right)$$
$$\times\Bigg\{ f_{K^*} m_{K^*}\left[g_\perp^{(v)}(u) - \frac{p^2}{2M^2} g_\perp^{(a)}(u)\right] q^2 + \frac{m_b f_{K^*}^\perp \phi_\perp(u)}{2u}(m_b^2 - q^2 - p^2 u^2)$$
$$+ f_{K^*} m_{K^*}\Bigg[\frac{(m_b^2 - q^2 - p^2u^2)}{2u}$$
$$\times\left(\Phi_\parallel(u) + u g_\perp^{(v)}(u) + \frac{(m_b^2 - q^2 - p^2u^2) g_\perp^{(a)}(u)}{4uM^2}\right)\Bigg]\Bigg\} \tag{7}$$

and

$$T_3(q^2) = \frac{1}{4}\left(\frac{m_b}{f_B m_B^2}\right)\exp\left(\frac{m_B^2}{M^2}\right)\int_\delta^1 \frac{\mathrm{u}}{u}\exp\left(-\frac{m_b^2 + p^2 u\bar{u} - q^2\bar{u}}{uM^2}\right)$$
$$\times\Bigg\{ m_{K^*} f_{K^*}\left[\frac{g_\perp^{(a)}(u)}{4} + \frac{(m_b^2 - q^2 - p^2u^2)}{4uM^2} g_\perp^{(a)}(u)\right]$$
$$- 2m_{K^*} f_{K*}\left[\frac{g_\perp^{(v)}(u)}{2}(2-u) - \frac{p^2 g_\perp^{(a)}(u)}{2M^2}\right]$$
$$+ 2m_{K^*} f_{K*}\Bigg[\frac{\Phi_\parallel(u)}{uM^2}\Bigg(\frac{m_b^2 - q^2 - p^2u^2}{u}$$
$$+ q^2 - M^2 + \frac{uM^2}{2}\Bigg)\Bigg] + m_b f_{K^*}^\perp \phi_\perp(u)\Bigg\}\,. \tag{8}$$

According to the light-cone sum rules derived in Ref. [17], the form factor A_0 is not independent but is given by

$$A_0(q^2) = \left(\frac{m_B + m_{K^*}}{2m_{K^*}}\right) A_1(q^2) + \left(\frac{q^2 - m_B^2 + m_{K^*}^2}{2m_{K^*}(m_B + m_{K^*})}\right) A_2(q^2)\,. \tag{9}$$

The above form factors depend on parameters related to the B meson, namely the Borel parameter M_B, the continuum threshold s_0^B, the quark mass m_b and the B meson decay constant f_B. Here we follow Ref. [17] and use the following set of parameter values : $M_B^2 = 8$ GeV^2, $s_0^B = 36$ GeV^2 and $m_b = 4.8$ GeV. We compute f_B using the sum rule given in Ref. [16] in order to reduce the sensitivity of the form factors to the b-quark mass [20]. The lower integration limit depends on the continuum threshold: $\delta = (m_b^2 - q^2)/(s_0^B - q^2)$. The function $\Phi_\parallel(u)$ is defined as

$$\Phi_\parallel(u) = \frac{1}{2}\left[\bar{u}\int_0^u \mathrm{v}\,\frac{\phi_\parallel(v)}{\bar{v}} - u\int_u^1 \mathrm{v}\,\frac{\phi_\parallel(v)}{v}\right] \tag{10}$$

and to leading twist-2 accuracy, $g_\perp^{(v)}(u)$ and $g_\perp^{(a)}(u)$ are also given in terms of the longitudinal twist-2 DA [20] :

$$g_\perp^{(v)}(u) = \frac{1}{2}\left[\int_0^u dv\, \frac{\phi_\parallel(v)}{\bar{v}} + \int_u^1 dv\, \frac{\phi_\parallel(v)}{v}\right] \tag{11}$$

and

$$g_\perp^{(a)}(u) = 2\left[\bar{u}\int_0^u dv\, \frac{\phi_\parallel(v)}{\bar{v}} + u\int_u^1 dv\, \frac{\phi_\parallel(v)}{v}\right] . \tag{12}$$

Therefore the form factors depend additionally on the longitudinal and transverse twist-2 DAs $\phi_{\parallel,\perp}$ of the K^* meson as well as its decay constants $f_{K^*}^\perp$ and f_{K^*} which we shall discuss in the next section.

III. ADS/QCD DISTRIBUTION AMPLITUDES

Traditionally, DAs are determined using QCD sum rules [21–24] which predict the moments of the DAs:

$$\langle \xi_{\parallel,\perp}^n \rangle_\mu = \int dz\, \xi^n \phi_{\parallel,\perp}(z,\mu) \tag{13}$$

where we have now made explicit the dependence of the DAs on the renormalization scale μ. In the standard sum rules approach, only the first two non-vanishing moments are available so that the sum rules DAs are reconstructed as truncated Gegenbauer polynomials:

$$\phi_{\parallel,\perp}(z,\mu) = 6z\bar{z}\left\{1 + \sum_{j=1}^{2} a_j^{\parallel,\perp}(\mu) C_j^{3/2}(2z-1)\right\} \tag{14}$$

where $C_j^{3/2}$ are the Gegenbauer polynomials and the coefficients $a_j^{\parallel,\perp}(\mu)$ are related to the moments $\langle \xi_{\parallel,\perp}^n \rangle_\mu$ [25]. These moments and coefficients are determined at a low scale $\mu = 1$ GeV and can then be evolved perturbatively to higher scales [24]. As $\mu \to \infty$, these coefficients vanish and the DAs take their asymptotic shapes.

Alternatively, the DAs can be obtained using AdS/QCD [15]. The AdS/QCD DAs are related to the light-front wavefunction of the K^* meson which can be obtained by solving the holographic light-front Schroedinger equation [26, 27] for mesons. In Ref. [15], we have shown that the twist-2 AdS/QCD DAs are given by

$$\phi_\parallel(z,\mu) = \frac{N_c}{\pi f_{K^*} m_{K^*}} \int dr\, \mu J_1(\mu r)[m_{K^*}^2 z(1-z) + m_f m_s - \nabla_r^2]\frac{\phi_L(r,z)}{z(1-z)} , \tag{15}$$

$$\phi_\perp(z,\mu) = \frac{N_c}{\pi f_{K*}^\perp} \int dr\, \mu J_1(\mu r)[m_s - z(m_s - m_{\bar{q}})]\frac{\phi_T(r,z)}{z(1-z)} \tag{16}$$

where $\phi_{\lambda=L,T}(r,z)$ are the AdS/QCD holographic light-front wavefunctions of the K^* meson and r the transverse distance between the quark and antiquark. Explicitly, the holographic wavefunction is given by [28]

$$\phi_\lambda(z,\zeta) = \mathcal{N}_\lambda \frac{\kappa}{\sqrt{\pi}} \sqrt{z(1-z)} \exp\left(-\frac{\kappa^2\zeta^2}{2}\right) \exp\left\{-\left[\frac{m_s^2 - z(m_s^2 - m_{\bar{q}}^2)}{2\kappa^2 z(1-z)}\right]\right\} \tag{17}$$

where $\zeta = \sqrt{z(1-z)}r$ is the light-front variable that maps onto the fifth dimension of AdS space [26]. The AdS/QCD wavefunction given by Eq. (17) is obtained using a quadratic [29, 30] dilaton in AdS in order to simulate confinement in physical spacetime. In that case, the parameter $\kappa = m_{K^*}/\sqrt{2}$. As discussed in reference [31], the normalization $\mathcal{N}_\lambda$ of the AdS/QCD wavefunction is fixed according to the polarization of the meson.

Note that both DAs are normalized, i.e.

$$\int_0^1 dz\, \phi_{\perp,\parallel}(z,\mu) = 1 \tag{18}$$

so that the decay constants are given by [15]

$$f_{K^*} = \frac{N_c}{m_{K^*}\pi} \int_0^1 dz\, [z(1-z)m_{K^*}^2 + m_{\bar{q}} m_s - \nabla_r^2] \frac{\phi_L(r,z)}{z(1-z)}\bigg|_{r=0} \tag{19}$$

and

$$f_{K^*}^\perp(\mu) = \frac{N_c}{\pi} \int_0^1 dz (m_s - z(m_s - m_{\bar{q}})) \int \mu J_1(\mu r) \frac{\phi_T(r,z)}{z(1-z)}\,. \tag{20}$$

We are thus able to make AdS/QCD predictions for the decay constants using Eqns. (19) and (20). Using constituent quark masses, i.e. $m_{\bar{q}} = 0.35$ GeV and $m_s = 0.48$ GeV, we obtain $f_{K^*} = 225$ MeV and $f_{K^*}^\perp(\mu) = 119$ MeV for $\mu \geq 1$ GeV. We point out that we choose constituent quark masses since they lead to a prediction for the ratio $f_{K^*}^\perp/f_{K^*}$ that is closest to the corresponding sum rules and lattice predictions [15]. Note also that our AdS/QCD DAs, shown in Fig. 1, also hardly depend on μ for $\mu \geq 1$ GeV.

IV. RESULTS

Having specified the DAs and decay constants, we are now in a position to compute the form factors using the light-cone sum rules given by Eqns. (3) to (8). In Figs. 2 to 8, we show our predictions for the seven form factors. In each figure, the solid blue curve is generated using our AdS/QCD DAs and decay constants. Restricting the AdS/QCD predictions to

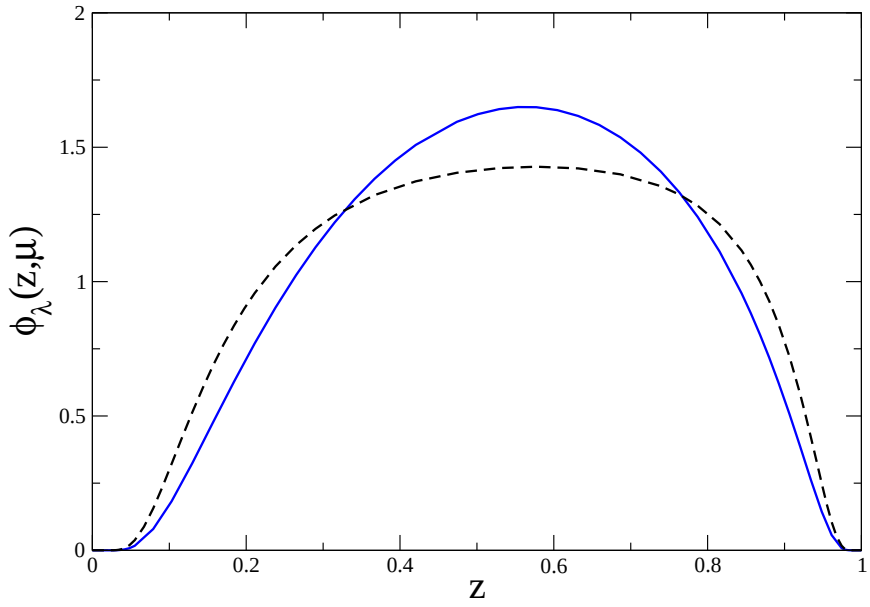

FIG. 1: The AdS/QCD twist-2 DAs. Solid blue: longitudinal ($\lambda = \|$) twist-2 DA. Dashed black: transverse ($\lambda = \perp$) twist-2 DA.

low-to-intermediate q^2 (in practice, we take $0 \leq q^2 \leq 16$ GeV^2) for each form factor, we fit the parametric form

$$F(q^2) = \frac{F(0)}{1 - a(q^2/m_B^2) + b(q^4/m_B^4)} \tag{21}$$

to our predictions. The fitted values of the parameters a and b are given in Table I and the resulting form factors are shown as the dashed red curves in Figs. 2 to 8. We repeat the fits by including the most recent unquenched lattice data of Ref. [19]. We use the data set obtained using the smallest lattice spacing. The fitted values of a and b are collected in Table II and the resulting form factors are shown as the dotted black curves in Figs. 2 to 8.

Finally we compute the differential branching fraction[36] given by [17]

F	$F(0)$	a	b
A_0	0.285	1.158	0.096
A_1	0.249	0.625	−0.119
A_2	0.235	1.438	0.554
V	0.277	1.642	0.600
T_1	0.255	1.557	0.499
T_2	0.251	0.665	−0.028
T_3	0.155	1.503	0.695

TABLE I: The values of the form factors at $q^2 = 0$ together with the fitted parameters a and b. The values of a and b are obtained by fitting Eq. (21) to the AdS/QCD predictions for low-to-intermediate q^2.

F	$F(0)$	a	b
A_0	0.285	1.314	0.160
A_1	0.249	0.537	−0.403
A_2	0.235	1.895	1.453
V	0.277	1.783	0.840
T_1	0.255	1.750	0.842
T_2	0.251	0.555	−0.379
T_3	0.155	1.208	−0.030

TABLE II: The values of the form factors at $q^2 = 0$ together with the fitted parameters a and b. The values of a and b are obtained by fitting Eq. (21) to both the AdS/QCD predictions for low-to-intermediate q^2 and the lattice data at high q^2.

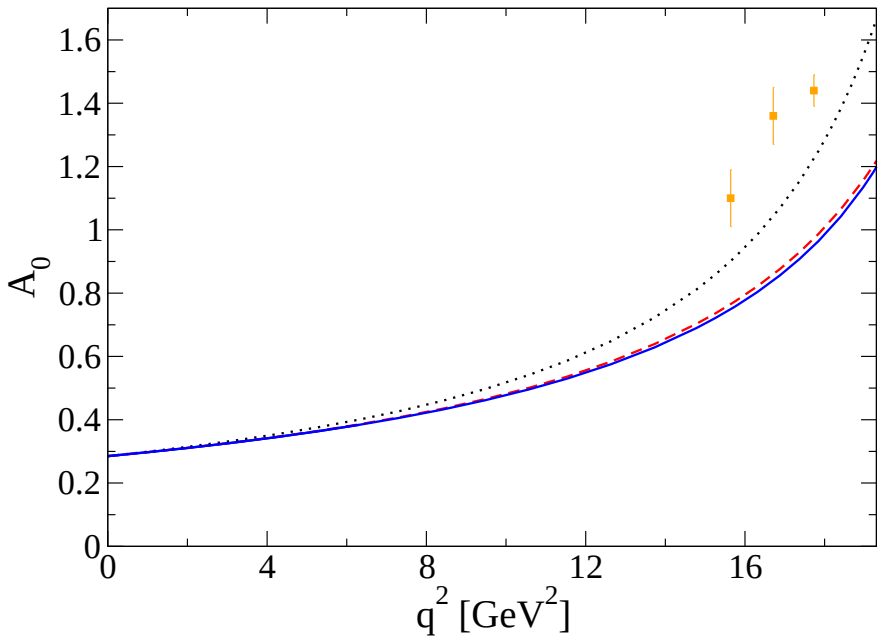

FIG. 2: The axial-vector form factor A_0. Solid blue: AdS/QCD. Dashed red: AdS/QCD Fit. Dotted black: Fit to AdS/QCD and lattice. Orange data points: lattice data.

$$\frac{d\mathcal{B}}{dq^2} = \tau_B \frac{G_F^2\alpha^2}{2^{11}\pi^5}\frac{|V_{tb}V_{ts}^*|^2\sqrt{\lambda}v}{3m_B}((2m_\mu^2+m_B^2 s)[16(|A|^2+|C|^2)m_B^4\lambda + 2(|B_1|^2+|D_1|^2)$$
$$\times\frac{\lambda+12rs}{rs} + 2(|B_2|^2+|D_2|^2)\frac{m_B^4\lambda^2}{rs} - 4[\Re\mathrm{e}(B_1B_2^*)+\Re\mathrm{e}(D_1D_2^*)]\frac{m_B^2\lambda}{rs}(1-r-s)]$$
$$+6m_\mu^2[-16|C|^2m_B^4\lambda + 4\Re\mathrm{e}(D_1D_3^*)\frac{m_B^2\lambda}{r} - 4\Re\mathrm{e}(D_2D_3^*)\frac{m_B^4(1-r)\lambda}{r} + 2|D_3|^2\frac{m_B^4 s\lambda}{r}$$
$$-4\Re\mathrm{e}(D_1D_2^*)\frac{m_B^2\lambda}{r} - 24|D_1|^2 + 2|D_2|^2\frac{m_B^4\lambda}{r}(2+2r-s)])$$

where $\lambda = 1+r^2+s^2-2r-2s-2rs$, with $r = m_K^2/m_B^2$ and $s = q^2/m_B^2$. The final muon has mass m_μ and velocity $v = \sqrt{1-4m_\mu^2/q^2}$. We take τ_B as the average of the lifetimes of the B° and B^+. The differential branching fraction depends on the following combinations of form factors:

$$A = C_9^{eff}\left(\frac{V}{m_B+m_{K^*}}\right) + 4C_7\frac{m_b}{q^2}T_1\ , \tag{22}$$

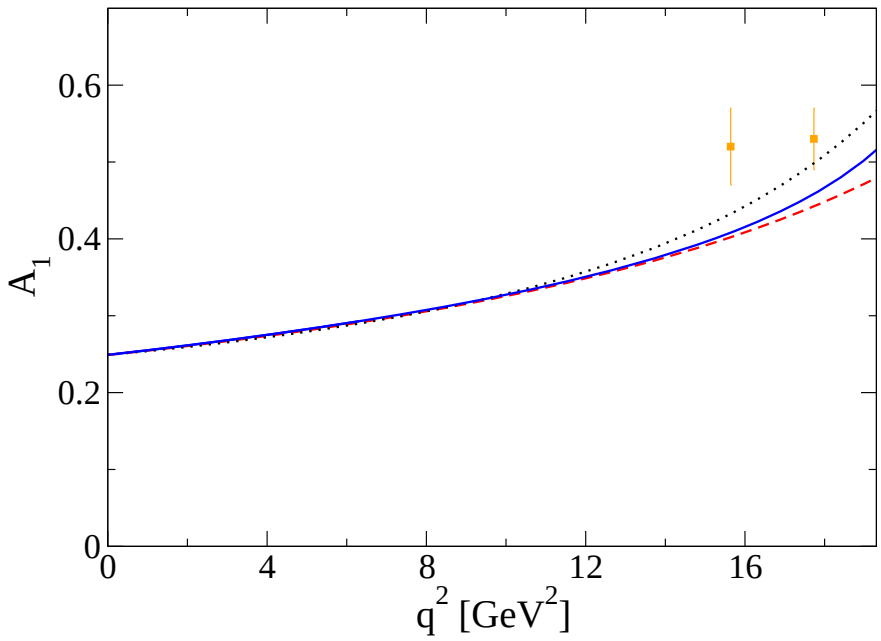

FIG. 3: The axial-vector form factor A_1. Solid blue: AdS/QCD. Dashed red: AdS/QCD Fit. Dotted black: Fit to AdS/QCD and lattice. Orange data points: lattice data.

$$B_1 = C_9^{eff}(m_B + m_{K^*})A_1 + 4C_7\frac{m_b}{q^2}(m_B^2 - m_{K^*}^2)T_2 \ , \tag{23}$$

$$B_2 = C_9^{eff}\left(\frac{A_2}{m_B + m_{K^*}}\right) + 4C_7\frac{m_b}{q^2}\left(T_2 + \frac{q^2}{m_B^2 - m_{K^*}^2}T_3\right) \ , \tag{24}$$

$$C = C_{10}\left(\frac{V}{m_B + m_{K^*}}\right) \ , \tag{25}$$

$$D_1 = C_{10}(m_B + m_{K^*})A_1 \ , \tag{26}$$

$$D_2 = C_{10}\left(\frac{A_2}{m_B + m_{K^*}}\right) \tag{27}$$

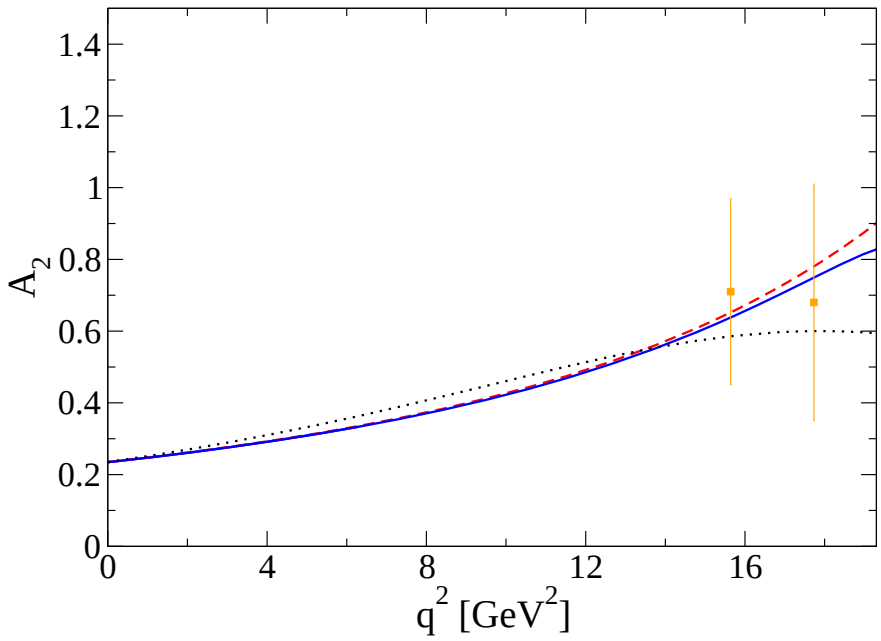

FIG. 4: The axial-vector form factor A_2. Solid blue: AdS/QCD. Dashed red: AdS/QCD Fit. Dotted black: Fit to AdS/QCD and lattice. Orange data points: lattice data.

and

$$D_3 = -C_{10}\frac{2m_{K^*}}{q^2}\left(\left(\frac{m_B + m_{K^*}}{2m_{K^*}}\right)A_1 - \left(\frac{m_B - m_{K^*}}{2m_{K^*}}\right)A_2 - A_0\right) \tag{28}$$

where $C_9^{eff} = C_9 + Y(q^2)$ with C_9, C_7 and C_{10} being the Standard Model Wilson coefficients given in Ref. [32] . The function $Y(q^2)$ is also given explicitly in Ref. [32].

In Fig. 9, we show our predictions for the differential branching ratio. The dashed red curve is generated by using the form factors that are fitted to only the AdS/QCD predictions. As can be seen, the curve somewhat overshoots the LHCb data at high q^2 especially in the $14\ \text{GeV}^2 \leq q^2 \leq 16\ \text{GeV}^2$ bin. Using the form factors that fit both the AdS/QCD predictions and the lattice data, we obtain the solid black curve. Rather surprisingly, adding the lattice data in our form factor fits worsens the disagreement at high q^2. However, this disagreement at high q^2 is consistent with the findings of Ref. [33] in the authors studied the possibility of new physics in the Wilson coefficients C_9 and C_9'. Indeed, by adding a negative new physics contribution, i.e. taking $C_9^{\text{NP}} = -1.5$ [9] (we keep $C_9' = 0$ as in the SM), we find a better fit to the data at high q^2as shown by the dot-dashed green curve of Fig. 9.

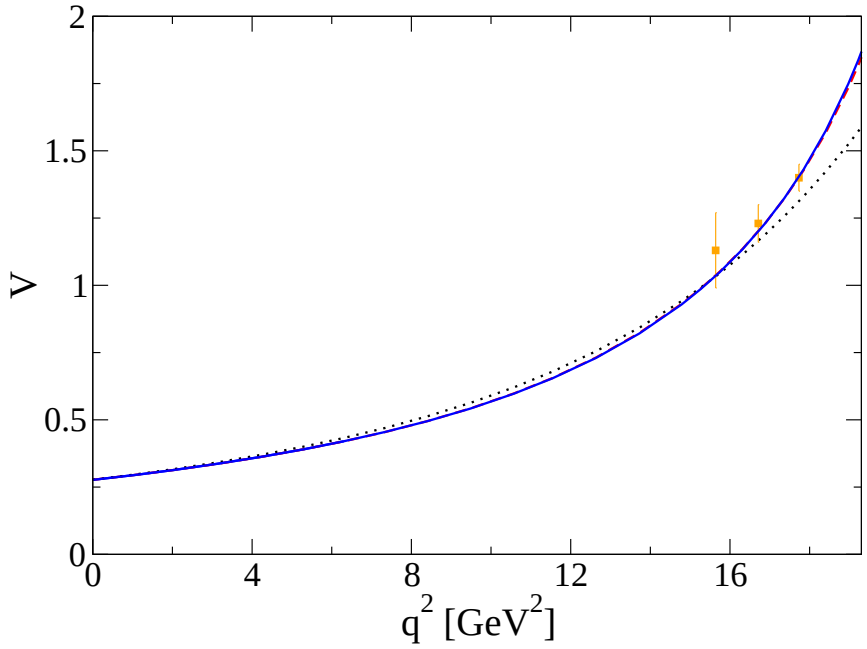

FIG. 5: The vector form factor V. Solid blue: AdS/QCD. Dashed red: AdS/QCD Fit. Dotted black: Fit to AdS/QCD and lattice. Orange data points: lattice data.

By integrating Eqn. (22) over q^2 and excluding the regions of the narrow charmonium resonances, we obtain a total branching fraction of $1.56 \times 10^{-6} (1.55 \times 10^{-6})$ when including (excluding) the lattice data compared to the LHCb measurement $(1.16 \pm 0.19) \times 10^{-6}$. In both cases, we overestimate the total branching fraction. With a new physics contribution to C_9, we obtain a total branching fraction of 1.35×10^{-6} in agreement with the LHCb data.

V. CONCLUSIONS

We have computed the seven $B \to K^*$ transition form factors using QCD light-cone sum rules with AdS/QCD DAs. We have provided two sets of parametrizations for the form factors: a first set that fits our AdS/QCD predictions at intermediate-to-high recoil and a second set that fits both our AdS/QCD predictions as well as the most recent lattice data at low recoil. The first set gives a good description of the data except at high q^2 where our prediction overshoots the data. The second set worsens the disagreement at high q^2. We

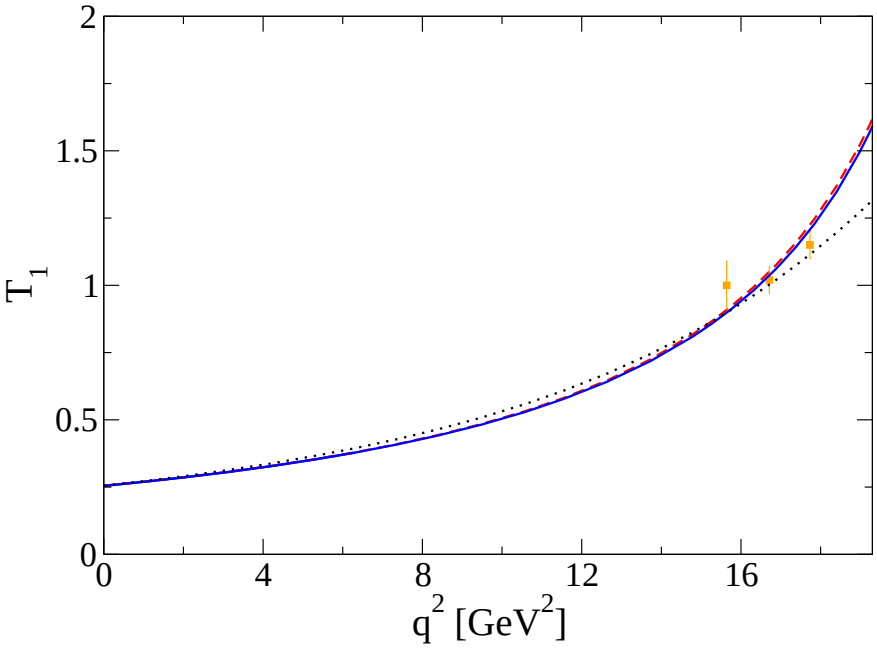

FIG. 6: The tensor form factor T_1. Solid blue: AdS/QCD. Dashed red: AdS/QCD Fit. Dotted black: Fit to AdS/QCD and lattice. Orange data points: lattice data.

looked into the possibility of a new physics contribution in the Wilson coefficient C_9 in order to improve agreement at high q^2.

VI. ACKNOWLEDGEMENTS

This research is supported by the Natural Sciences and Engineering Research Council of Canada (NSERC). We thank T. Aliev and M. Wingate for useful correspondence.

[1] T. Aaltonen et al. (CDF Collaboration), Phys.Rev.Lett. **108**, 081807 (2012), 1108.0695.

[2] J. Lees et al. (BaBar Collaboration), Phys.Rev. **D86**, 032012 (2012), 1204.3933.

[3] J.-T. Wei et al. (BELLE Collaboration), Phys.Rev.Lett. **103**, 171801 (2009), 0904.0770.

[4] R. Aaij et al. (LHCb collaboration), Phys.Rev.Lett. **111**, 191801 (2013), 1308.1707.

[5] R. Aaij et al. (LHCb Collaboration), JHEP **1207**, 133 (2012), 1205.3422.

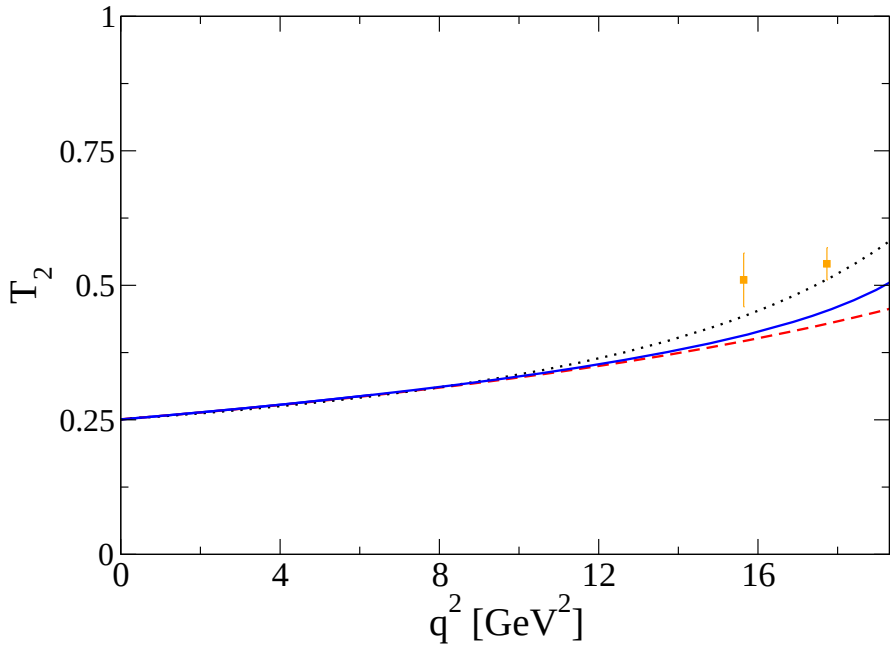

FIG. 7: The tensor form factor T_2. Solid blue: AdS/QCD. Dashed red: AdS/QCD Fit. Dotted black: Fit to AdS/QCD and lattice. Orange data points: lattice data.

[6] R. Aaij et al. (LHCb Collaboration), JHEP **1308**, 131 (2013), 1304.6325.

[7] (2012), linked to LHCb-ANA-2011-089.

[8] W. Altmannshofer and D. M. Straub (2013), 1308.1501.

[9] S. Descotes-Genon, J. Matias, and J. Virto, Phys.Rev. **D88**, 074002 (2013), 1307.5683.

[10] T. Hurth and F. Mahmoudi (2013), 1312.5267.

[11] S. Descotes-Genon, T. Hurth, J. Matias, and J. Virto, JHEP **1305**, 137 (2013), 1303.5794.

[12] R. Gauld, F. Goertz, and U. Haisch (2013), 1308.1959.

[13] A. J. Buras and J. Girrbach, JHEP **1312**, 009 (2013), 1309.2466.

[14] R. Gauld, F. Goertz, and U. Haisch (2013), 1310.1082.

[15] M. Ahmady and R. Sandapen, Phys.Rev.D **88**, 014042 (2013), 1305.1479.

[16] A. Ali, V. M. Braun, and H. Simma, Z.Phys. **C63**, 437 (1994), hep-ph/9401277.

[17] T. Aliev, A. Ozpineci, and M. Savci, Phys.Rev. **D56**, 4260 (1997), hep-ph/9612480.

[18] P. Ball and R. Zwicky, Phys.Rev. **D71**, 014029 (2005), hep-ph/0412079.

[19] R. R. Horgan, Z. Liu, S. Meinel, and M. Wingate (2013), 1310.3722.

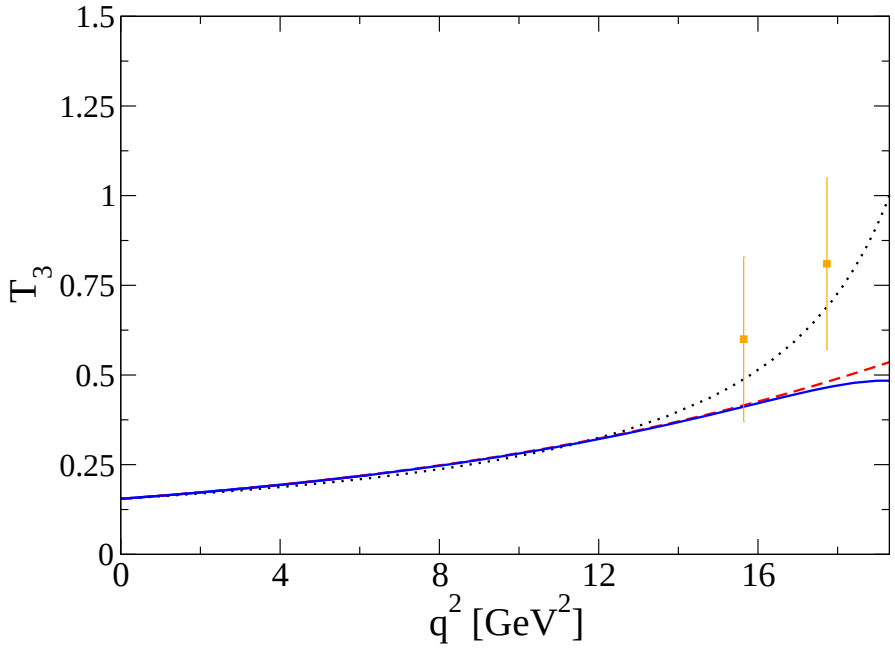

FIG. 8: The tensor form factor T_3. Solid blue: AdS/QCD. Dashed red: AdS/QCD Fit. Dotted black: Fit to AdS/QCD and lattice. Orange data points: lattice data.

[20] P. Ball and V. M. Braun, Phys.Rev. **D55**, 5561 (1997), hep-ph/9701238.

[21] P. Ball and V. M. Braun, Phys. Rev. **D54**, 2182 (1996), hep-ph/9602323.

[22] P. Ball and V. M. Braun (1998), hep-ph/9808229.

[23] P. Ball and V. M. Braun, Nucl. Phys. **B543**, 201 (1999), hep-ph/9810475.

[24] P. Ball, V. M. Braun, and A. Lenz, JHEP **08**, 090 (2007), 0707.1201.

[25] H.-M. Choi and C.-R. Ji, Phys. Rev. **D75**, 034019 (2007), hep-ph/0701177.

[26] G. F. de Teramond and S. J. Brodsky, Phys.Rev.Lett. **102**, 081601 (2009), 0809.4899.

[27] S. J. Brodsky and G. F. de Teramond, AIP Conf.Proc. **1116**, 311 (2009), 0812.3192.

[28] A. Vega, I. Schmidt, T. Branz, T. Gutsche, and V. E. Lyubovitskij, Phys.Rev. **D80**, 055014 (2009), 0906.1220.

[29] S. J. Brodsky, G. F. de Teramond, and H. G. Dosch (2013), 1302.4105.

[30] S. J. Brodsky, G. F. de Teramond, and H. G. Dosch (2013), 1302.5399.

[31] J. R. Forshaw and R. Sandapen, Phys.Rev.Lett. **109**, 081601 (2012), 1203.6088.

[32] W. Altmannshofer, P. Ball, A. Bharucha, A. J. Buras, D. M. Straub, et al., JHEP **0901**, 019

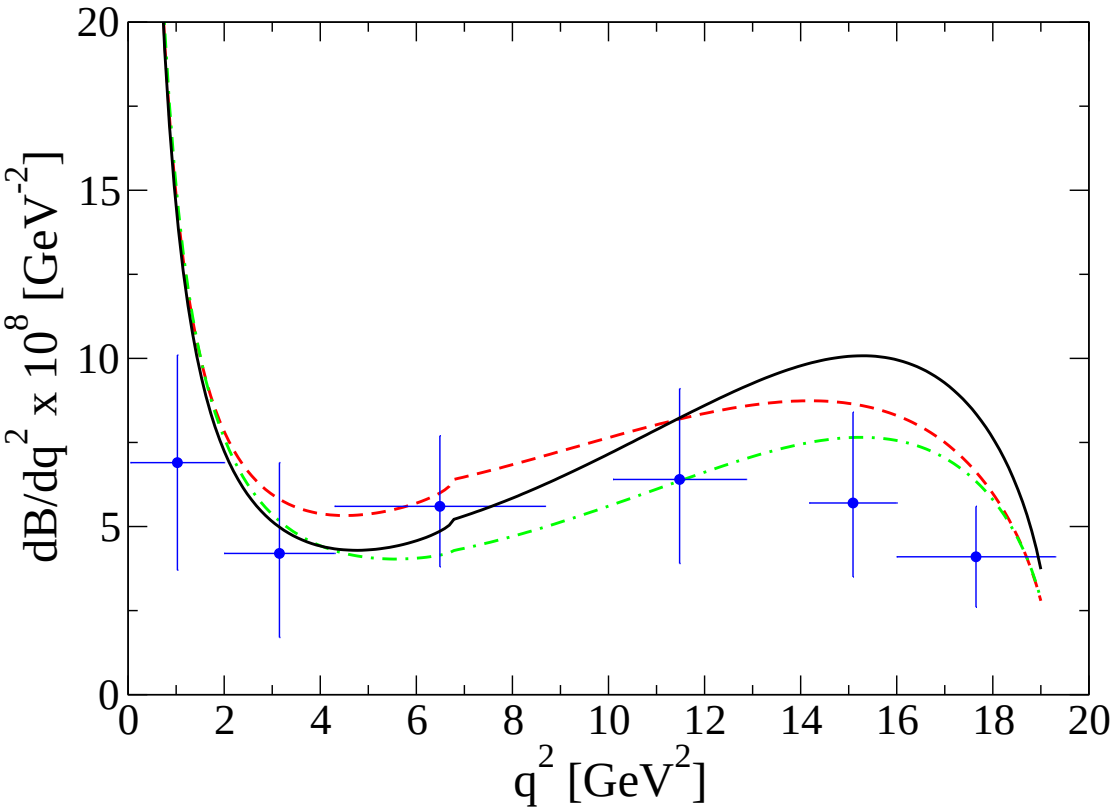

FIG. 9: The differential branching fraction as a function of q^2. For the LHCb data, we average over the data for $B^+ \to K^{*+}\mu^+\mu^-$ given in Ref. [5] and the data for $B^\circ \to K^{*\circ}\mu^+\mu^-$ given in Ref. [7]. Dashed red : AdS/QCD fit. Solid black: AdS/QCD + lattice fit. Dot-dashed green: AdS/QCD + lattice + NP in the Wilson coefficient C_9.

(2009), 0811.1214.

[33] R. R. Horgan, Z. Liu, S. Meinel, and M. Wingate (2013), 1310.3887.

[34] M. Ahmady, R. Campbell, S. Lord, and R. Sandapen, Phys.Rev. **D88**, 074031 (2013), 1308.3694.

[35] A recent computation of the $B \to \rho$ form factors can be found in Ref. [34].

[36] We have summed over the two possible final lepton polarizations.